# Radiative lifetimes and cooling functions for astrophysically important molecules

**Jonathan Tennyson[1,2], Kelsey Hulme[1], Omree K. Naim[1] and Sergei N. Yurchenko[1]**

[1]Department of Physics & Astronomy, University College London, Gower St., London, WC1E 6BT, UK

E-mail: [2]j.tennyson@ucl.ac.uk

**Abstract.**

Extensive line lists generated as part of the ExoMol project are used to compute lifetimes for individual rotational, rovibrational and rovibronic excited states, and temperature-dependent cooling functions by summing over all dipole-allowed transitions for the states concerned. Results are presented for SiO, CaH, AlO, ScH, $H_2O$ and methane. The results for $CH_4$ are particularly unusual with 4 excited states with no dipole-allowed decay route and several others where these decays lead to exceptionally long lifetimes. These lifetime data should be useful in models of masers and estimates of critical densities, and can provide a link with laboratory measurements. Cooling functions are important in stellar and planet formation.

## 1. Introduction

There are vast areas of the Universe where molecules exist at very low temperatures. However molecules actually occur in a wide variety of environments many of them significantly hotter including planetary nebulae, atmospheres of (exo-)planets, brown dwarfs and cool stars. This makes the radiative and cooling properties of the molecules important for models of these species. Indeed, although interstellar molecular clouds are usually characterised as cold, they are not really fully thermalised. Whether a species, or state of that species, is thermalised depends on the critical density which is given by the ratio of the radiative lifetime of the state to the rate for collisional excitation to the state. In such regions radiative lifetimes are also important for models of the many species which are observed to mase. The long lifetimes associated with certain excited states can lead to population trapping and non-thermal distributions. Such behaviour has been observed for the $H_3^+$ molecule both in space (Goto et al. 2002, Oka et al. 2005) and the laboratory (Krechel et al. 2002, Kreckel et al. 2004), in both cases leading to state distributions which had not been anticipated.

States with short radiative lifetimes are important for direct laser cooling of polar diatomic molecules, a topic which has recently attracted significant interest (Shuman et al. 2010).

Cooling functions are important in a variety of environments. For example cooling by $H_3^+$ is known to be important in the atmospheres of solar system gas giants (Schwalm et al. 2011) and, it has been suggested, vital to stability of so-called "hot Jupiter" exoplanets (Koskinen et al. 2007). Similarly, cooling functions are important in the primordeal Universe for the formation of the first stars (Abel et al. 2002) and galaxies (Benson 2010, Bromm et al. 2009). At temperatures below about 8000 K, this cooling is almost entirely provided by molecules (Miller et al. 2010). Although cooling functions are available for some key diatomics (Coppola et al. 2011) and there have been several attempts to provide cooling functions for $H_3^+$ (Neale et al. 1996, Miller et al. 2010, Miller et al. 2013), there are no systematic compilations of these. Indeed cooling functions for many key species, such as water, do not appear to be available.

The ExoMol project (Tennyson & Yurchenko 2012) has been undertaking the systematic calculation of very extensive spectroscopic line lists for molecules deemed to be important for the study of exoplanet and other hot atmospheres. These line lists provide comprehensive datasets of a molecule's radiative properties. Here we use these datasets to systematically study radiative lifetimes of comprehensive sets of states and to compute temperature-dependent cooling functions for molecules considered as part of the ExoMol project.

## 2. Theory

The results of ExoMol calculations have, up until now, been stored in two files (Tennyson et al. 2013): a states file comprising one, numbered line per state which gives the energy

level of the state plus associated quantum numbers, and a transitions file with gives a list of Einstein A coefficients, $A_{if}$, plus the numbers of the initial, $i$, and final, $f$, states which, in turn, refer back to the states file. The lifetime of state $i$, $\tau_i$, can be computed by summing over A coefficients:

$$\tau_i = \frac{1}{\sum_f A_{if}} \ . \tag{1}$$

This is in principle straightforward, although the sheer size of some of the transitions files, which can contain many billions of entries (Yurchenko & Tennyson 2014, Sousa-Silva et al. 2015, Pavlyuchko et al. 2015*a*), does mean that the data handling requires some care.

At temperature $T$, the cooling function, $W(T)$, is the total energy emitted by a molecule and is given by

$$W(T) = \frac{1}{4\pi Q(T)} \sum_{i,f} A_{if} hc\nu_{if} (2J_i + 1) g_i \exp\left(\frac{-c_2 \tilde{E}_i}{T}\right) \tag{2}$$

where $\nu_{if}$ is the wavenumber of the transition $i \rightarrow f$, $J_i$ is the rotational quantum number of the initial state and $g_i$ is its nuclear spin degeneracy factor. The final, exponential term is the Boltzmann factor for which we use the second radiation constant, $c_2 = 1.43877736$ cm K, since ExoMol actual stores energies $\tilde{E}$ as wavenumbers in cm$^{-1}$. Finally, $Q(T)$ is the partition function given by

$$Q(T) = \sum_i (2J_i + 1) g_i \exp\left(\frac{-c_2 \tilde{E}_i}{T}\right). \tag{3}$$

Partition functions are computed routinely for each molecule studied by the ExoMol project.

The general procedure used by ExoMol to produce linelists is to use potential energy curves and surfaces obtained by refining high quality *ab initio* curves and surfaces using spectroscopic data. Wavefunctions are obtained using variational nuclear motion codes (Tennyson et al. 2004, Le Roy 2007, Yurchenko et al. 2007, Pavlyuchko et al. 2015*b*, Yurchenko, Lodi, Tennyson & Stolyarov 2015). Conversely dipole moment curves and surfaces are obtained *ab initio*: experience has shown that, at least for molecules containing light atoms, these are capable of giving results as accurate as the best measurements (Lodi et al. 2011, Polyansky et al. 2015).

## 3. Results: lifetimes

Lifetimes were obtained for molecules treated by the ExoMol project (Tennyson & Yurchenko 2016). Examples are analysed below with complete sets of data being placed on the ExoMol website (www.exomol.com). While the ExoMol line lists are very extensive, with a few exceptions (Engel et al. 2005, Kyuberis et al. 2016), they are not complete. Instead the project aims to provide comprehensive line lists which

are effectively complete for a given upper temperature and range of wavelengths. These choices vary with the expected stability of a given species but typical objectives are the provision of a line list which represents all absorbtion longwards of 1 $\mu$m (at wavenumbers below 10 000 cm$^{-1}$) for temperatures up to 3000 K. In general these parameter ranges are increased for diatomics species which may be stable in environments as hot as our Sun's photosphere (almost 6000 K) and for which absorptions at visible wavelengths are of importance. Conversely, for large molecules such as nitric acid ($HNO_3$) the range of temperatures considered is significantly reduced, to only 500 K in this case (Pavlyuchko et al. 2015*a*). These choices are partially influenced by practical considerations as calculations on polyatomic systems become very computationally expensive (Yurchenko & Tennyson 2014). These considerations influence the states for which lifetime data is presented below.

By definition the ground state of all systems considered has an infinite lifetime to radiative decay. Some excited states also do not have allowed radiative decay routes, for example where these are forbidden by nuclear spin considerations. In principle, radiative nuclear spin transitions which interchange ortho and para nuclear spin isomers can occur but they are extremely weak (Miani & Tennyson 2004) and such transitions are not considered as part of ExoMol. States whose lifetimes are computed to be infinite are not considered below. In the following subsections we present lifetime results for a series of molecules starting with diatomics, ordered by the complexity of their electronic structure, and followed by the polyatomic molecules water and methane.

### *3.1. SiO*

The ExoMol project has provided line lists for a number of closed shell diatomic species including NaCl and KCl (Barton et al. 2013), PN (Yorke et al. 2014), NaH (Rivlin et al. 2015), CS (Paulose et al. 2015) and CaO (Yurchenko, Blissett, Asari, Vasilios, Hill & Tennyson 2015). For NaH and CaO these studies also considered electronically excited state. Here we consider SiO as an example. The silicon monoxide linelists of Barton et al. (2013) are particularly comprehensive, considering all vibrational and rotational level up to the electronic ground state, corresponding to $v \leq 98$ and $J \leq 423$. They are expected to be complete for temperatures up to 9000 K and considered wavelenghts much shorter than 1 $\mu$m. We note that these very weak, short wavelength transitions are likely to be subject to numerical problems (Li et al. 2015, Medvedev et al. 2015) which, however, are not expected to influence the results presented below. In addition, SiO is a well-studied maser whose emissions have been observed in a variety of sources and at several wavelengths (Gray 1999, Deguchi et al. 2004, McIntosh & Hayes 2008, Cho et al. 2009, Li et al. 2010, Cotton et al. 2010).

Figure 1 gives lifetimes for vibration-rotation states of $^{28}Si^{16}O$. In general these lifetimes vary smoothly with vibrational state, $v$, and rotational state, $J$, showing reduced lifetimes upon excitation of either mode. States in the $v = 0$ vibrational ground state can only decay by a single, $\Delta J = 1$, transition. The rigid rotor approximation

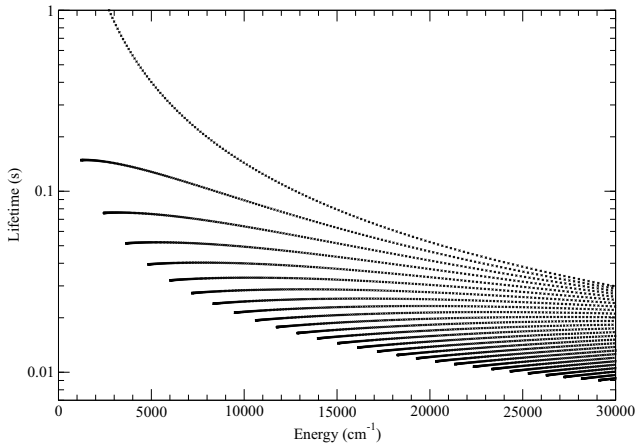


**Figure 1.** Lifetimes of the vibration-rotation states of $^{28}Si^{16}O$. From the top the curves are for vibrational state $v = 0$, $v = 1$ up to $v = 27$. Curves comprise states of increasing rotational quantum number, $J$, with energy. State with $J \leq 61$ for $v = 0$ are too long-lived to fit in the figure and are discussed in the text.

suggests that such decays should lead to lifetimes which depend on $J^{-3}$ and this behaviour is followed by our results. This means that the first excited state with $J = 1$ has a long lifetime, which we compute to be $3.32 \times 10^5$ s.

The lifetimes of the vibrational-rotation states of other closed shell diatomic molecules we studied behave in a similar fashion.

### *3.2. CaH*

ExoMol has considered the vibration-rotation spectrum for a number of molecules whose electronic state also contains angular momentum (Yadin et al. 2012). In this case it is necessary to consider a variety of couplings which are not present in a non-relativistic, Born-Oppenheimer treatment of the problem such as spin-orbit, spin-spin and spin-rotation coupling. Here we consider calcium mononhydride, CaH, as an example.

The electronic ground state of calcuim monohydride has $^2\Sigma^+$ symmetry. A line list for it was computed by Yadin et al. (2012) with $v \leq 19$ and $J \leq 74$. We note that an alternative line list, which also considered transitions to the first 5 electronic states, has been provided by (Weck et al. 2003); this line list, which is purely *ab initio*, did not consider fine structure and other coupling effects.

Figure 2 summarises our results. The figure shows a number of features broadly in line with those seen for SiO above: for example lifetimes for the $v = 0$ levels again showing a $J^{-3}$ behaviour. For higher $J$ values there appears to be little dependence on spin component. However this is not true at low $J$ where it is found that the lifetimes for the higher, $f$, component increase while those for the lower $e$ component decrease significantly.

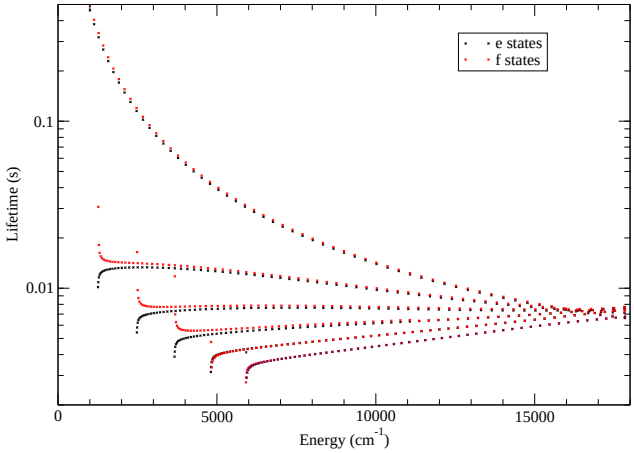


**Figure 2.** Lifetimes of the vibration-rotation states of $^{40}$CaH. From the top the "curves" are for vibrational state $v = 0$, $v = 1$ up to $v = 5$. Each vibrational curves is actually a doublet with the generally longer-lived component representing the $f$-states in red and the shorter-lived $e$-states being given in black.

### *3.3. AlO*

Aluminium monoxide is chosen not only because it is an important astronomical species having been observed in sunspots (Sriramachandran et al. 2013) and a variety of other stars (Kaminski et al. 2013, Banerjee et al. 2004, Banerjee et al. 2012) but also for terrestrial applications were emissions arise from rocket exhausts (Knecht et al. 1996) and plasmas (Surmick & Parigger 2014). Furthermore there are direct experimental measurements of radiative lifetimes for vibrational levels in the B $^2\Sigma^+$ state (Johnson et al. 1972, Dagdigian et al. 1975).

The ExoMol model for AlO considered the three lowest electronic states, all of which are spin doublets: X $^2\Sigma^+$, A $^2\Pi$ and B $^2\Sigma^+$. In practice the X and A states are close together and cross at energies under consideration leading to significant interaction between the states which is explicitly allowed for in the model used (Patrascu et al. 2014). Lifetimes for AlO were computed using the linelist of Patrascu et al. (2015) which considered ($v \leq 66, J \leq 300.5$), ($v \leq 63, J \leq 300.5$) and ($v \leq 40, J \leq 232.5$) for the X, A and B states respectively. This linelist is designed to be valid for temperatures up to 8000 K and considered states as high as 40 000 cm$^{-1}$. However above 30 000 cm$^{-1}$ the line list does not include all transitions meaning that for states in this region the computed some lifetimes are artificially long; thus only states below 30 000 cm$^{-1}$ are considered.

Figure 3 gives an overview of lifetimes of levels belonging to the lowest three electronic states of $^{27}$Al$^{16}$O. Broadly, the curves in the top left are associated with levels belonging to the X $^2\Sigma^+$ ground state, the large clump in the middle belong to the low-lying A $^2\Pi$ state and the short lived levels at higher energy belong to the B $^2\Sigma^+$ state.

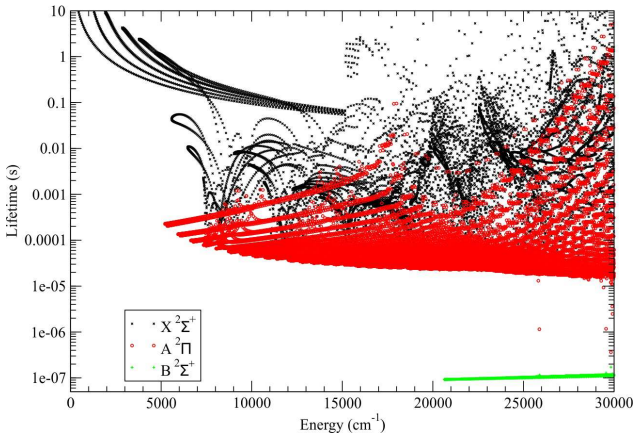


**Figure 3.** Overview of lifetimes for states of $^{27}Al^{16}O$.

Superficially the structure of the X $^2\Sigma^+$ state lifetimes are similar to those discussed above for SiO. However they differ in two key aspects, firstly the states are much longer lived and secondly the shortest lived curve is for levels with $v = 0$ and lifetimes actually increase with vibrational excitation. These features are due to the very flat dipole moment curve of AlO which leads to unusually weak vibrational transitions (Lengsfield & Liu 1982, Patrascu et al. 2015).

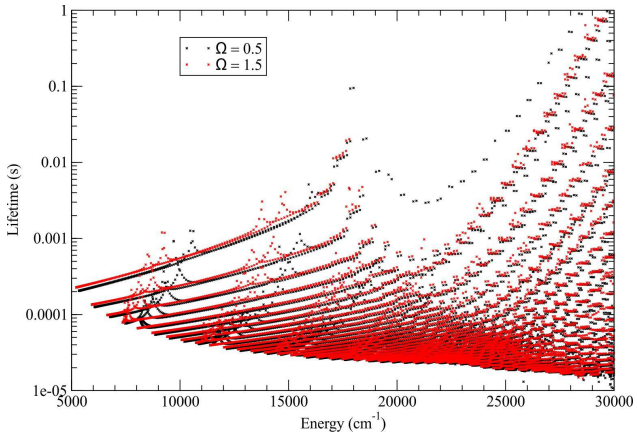


**Figure 4.** Lifetimes of the vibration-rotation states of A $^2\Pi$ of AlO.

The lifetimes of levels associated with the A $^2\Pi$ state vary by many orders of magnitude. This is partly due to interaction with much longer-lived levels from the X $^2\Sigma^+$ state via spin-orbit coupling; the mixing of the wavefunctions between the two states leads to many structures in the lifetimes plot. Furthermore the A $^2\Pi$ state itself is split into $\Omega = \frac{1}{2}$ and $\Omega = \frac{3}{2}$ states by spin-orbit coupling. As shown in Fig. 4, the lifetimes of levels associated with these curves are rather similar except when the levels interact with levels associated with the X $^2\Sigma^+$ state.

There available measurements of lifetimes for the $v = 0$, 1 and 2 levels of the B $^2\Sigma^+$ state: Johnson et al. (1972) obtained $128 \pm 6$, $125 \pm 5$ and $130 \pm 7$ ns respectively for these levels while Dagdigian et al. (1975) obtained $100 \pm 7$, $102 \pm 7$ and $102 \pm 4$ ns respectively. These measurements were both rotationally unresolved for unspecified rotational distributions. Figure 5 shows our rotationally resolved results for the lowest 10 vibrational states of the B $^2\Sigma^+$ state. It is clear that our calculations reproduce the trend of slowly increasing lifetime with vibrational state. The calculations also suggest that the lifetimes increase with rotational excitation making our results agree with those of Dagdigian et al. (1975) for $J$ in the region of 85 and those of Johnson et al. (1972) for somewhat higher values of $J$.

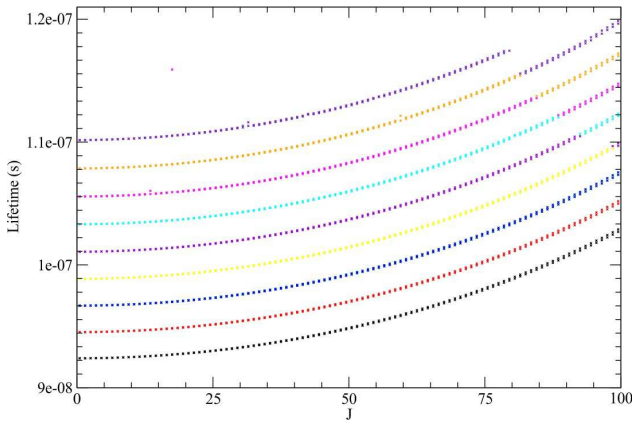


**Figure 5.** Lifetimes of the vibration-rotation states of B $^2\Sigma^+$ of AlO. From bottom to top the curves are for vibrational state $v = 0$, $v = 1$ up to $v = 9$. The small splittings visible at higher $J$s is due to spin-rotation effects.

### *3.4. ScH*

Figure 6 shows scandium monohydride lifetimes calculated using the linelist of Lodi et al. (2015) which considered the lowest six levels of ScH and $J \leq 59$. In energy order these states are the X $^1\Sigma^+$ ground electronic state, a $^3\Delta$, b $^3\Pi$, A $^1\Delta$, B $^1\Pi$, and c $^3\Sigma^+$. The minima of these states span a range of little more than 6000 cm$^{-1}$. The many overlaps and couplings between these states causes a complicated set of patterns in the lifetime plot.

In contrast to the systems considered above, the model for ScH contains electronic states with different spin symmetries. In particular, while the ground state is a singlet, the first excited state is a triplet meaning that there is no dipole connecting the two states. The a $^3\Delta$ state is therefore metastable and its levels have long lifetimes.

Unlike the other systems considered here, the line list computed by Lodi et al. (2015) for ScH is completely *ab initio* since there was insufficient available spectroscopic

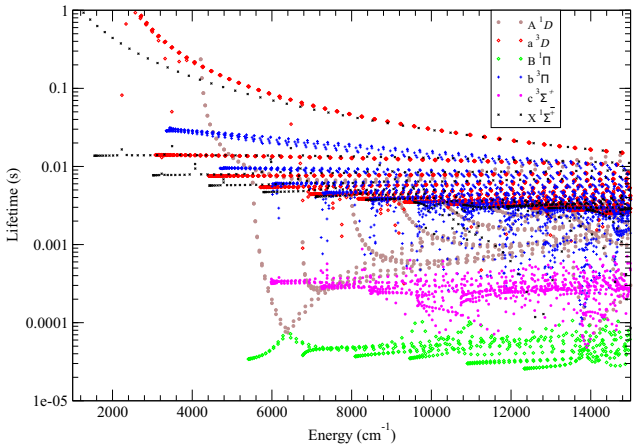


**Figure 6.** Lifetimes for states of $^{45}$ScH.

data to refine the *ab initio* model. In addition, experience has shown that present state-of-the-art *ab initio* calculations give a much poorer starting point in transition metal containing molecules. This means that our results for ScH must be regarded as highly uncertain. Some experimentally measured lifetimes for this system would be very helpful as input to an improved model.

### *3.5. Water*

In contrast to molecules like ScH and AlO, the intensity of key astrophysical transitions for a molecule like water are both well studied and well-known (Barber et al. 2006, Rothman et al. 2013). However, as we show below, the lifetimes of the various levels of water do not follow the simple patterns of, say, SiO discussed above. The lifetimes are important for models of the many water masers lines found both in ground (Neufeld & Melnick 1991) and excited (Hirota et al. 2012) vibrational states as they can affect the pumping routes and level populations that lead to inversions. Indeed the water maser is a textbook example (Gray 2012). Similar considerations apply to fluorescence from comets (Dello Russo et al. 2004, Dello Russo et al. 2005).

Here we use the BT2 line list of Barber et al. (2006) whose construction actually pre-dated the ExoMol project. BT2 considered all states of water up to 30 000 cm$^{-1}$ with $J \leq 50$ and contains over 500 million transitions.

Figure 7 plots the lifetimes for levels lying below 5000 cm$^{-1}$; ortho and para levels are denoted separately since these species effectively behave as separate molecules. While the general structure of lifetimes is similar to that discussed for SiO, it is clear that the rotational substructure introduces additional complications. Indeed lifetimes for levels with the same total rotational quantum, $J$, within the vibrational ground state can differ by up to an order of magnitude. While the shorter-lived levels, which include the so-called water backbone (Gray 2012) important for maser models, show

some systematic structure in their lifetimes and similar values for ortho and para species, the variation between the lifetimes of the longer-lived levels is significant. It is the details of this structure which allow masing to occur: for example when the lifetime of the higher level is significantly longer relative to the lower, the upper level can overpopulate relative to the lower, critical for masing to occur.

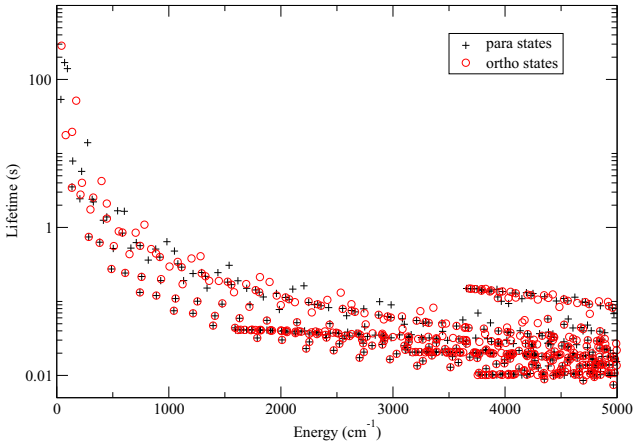


**Figure 7.** Lifetimes of the vibration-rotation states of $H_2{}^{16}O$.

## 4. Methane

Methane is an important astronomical molecule and easily detected in hot environments (Yurchenko et al. 2014), but it does not possess a permanent dipole moment hindering its detection in interstellar environments (Lacy et al. 1991). However, methane does possess a weak rotational spectrum (Cole & Honey 1975, Oldani et al. 1985, Hilico et al. 1997, Boudon et al. 2010) which is important for studies of methane in giant planets and Titan (Wishnow et al. 2007). Lifetimes were computed using the 10to10 line list of Yurchenko & Tennyson (2014) which contains almost 10 billion vibration-rotation transitions with $J \leq 39$.

The high symmetry of $CH_4$ brings some unusual features to its spectroscopic behaviour. Nuclear spin statistics divides the levels into three distinct groups conventionally known as ortho, meta and para. One might expect that there would thus be 3 levels which do not undergo dipole-allowed radiative decay corresponding to the lowest level of each group. In fact, there are seven such levels. Labelling them as $(J, n$,symmetry), where $n$ is simply a counting number, they are the lowest ortho state (0,1,$A_1$) at 0 cm$^{-1}$, the lowest meta level (1,1,$F_1$) at 10.48 cm$^{-1}$, and the lowest para level (2,1,E) at 31.44 cm$^{-1}$, which are the lowest three levels in the molecule. In addition the three ortho states (3,1,$A_2$) at 62.88 cm$^{-1}$, (6,1,$A_2$) at 219.92 cm$^{-1}$ and (9,1,$A_1$) at 470.84 cm$^{-1}$ and the para state (4,1,E) at 104.78 cm$^{-1}$ do not have any dipole allowed

transitions linking them to lower levels. These states will probably decay slowly by other means, such as via electric quadrupole transitions.

Figure 8 gives lifetimes of vibration-rotation states of methane lying below 4000 $cm^{-1}$. The very weak nature of methane's rotational spectrum means that states with no vibrational excitation live for a long time and the figure actually spans 14 orders of magnitude. In fact there are three very long-lived states which are omitted from the figure. These are (3,1,$F_2$) at 62.88 $cm^{-1}$, (6,1,$A_1$) at 219.95 $cm^{-1}$ and (12,1,$A_2$) at 817.10 $cm^{-1}$. None of these states can undergo a dipole-allowed P ($\Delta J = -1$) transition and instead each decay via a single, very long-wavelength Q ($\Delta J = 0$) transition. Our calculated lifetimes are $1 \times 10^{23}$, $4 \times 10^{17}$, and $6 \times 10^{13}$ s, respectively. These are huge: in particular the lifetime of the (3,1,$F_2$) is predicted to be a thousand times the age of the Universe! Our precise numbers are rather uncertain because the lifetime depends on the cube of the wavelength which, for close-by energy levels, is calculated with a significant uncertainty. Furthermore, given the long lifetimes, it is likely that other non-dipole or two photon decays may become dominant. However, the prediction that these three states are very long-lived in collision-free environments is likely to be correct. The very faint, pure rotational spectrum of methane has been studied by Boudon et al. (2010), who were able to determine values for the very small dipoles linking the rotational states. It is the small values of these transition dipoles combined with the small gap between the states involved that leads to the exceptionally long radiative lifetimes for certain states.

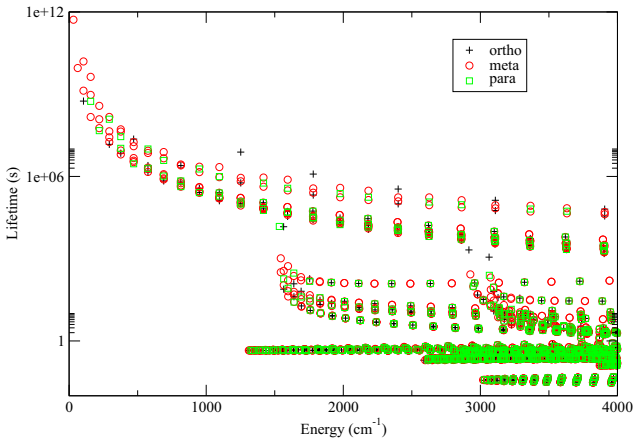


**Figure 8.** Lifetimes of the vibration-rotation states of $^{12}CH_4$.

## 5. Cooling functions

Cooling functions were computed for the molecules discussed above using the same line lists. Results are given here graphically, see Fig. 9 and 10, and are given numerically in 1 K intervals on the ExoMol website. The cooling functions of AlO and ScH show

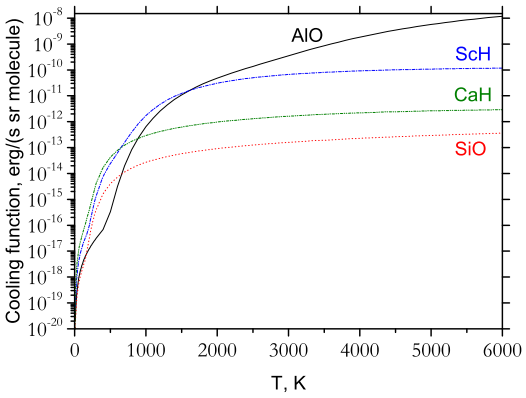


**Figure 9.** Temperature-dependent cooling functions for $^{40}$CaH, $^{28}$Si$^{16}$O, $^{27}$Al$^{16}$O and $^{45}$ScH.

structure at lower temperatures due to the presence of transitions from exited electronic states. The strong electronic transitions also lead to the cooling functions for these two molecules being significantly stronger, especially of AlO at $> 2000$ . The cooling function for water was computed up to $T$=3000 K, which is the temperature limit of the BT2 linelist used (Barber et al. 2006) and that for methane up to $T$=1500 K, the limit for the 10to10 list. Methane is actually a rather inefficient cooler below about 500 K which can be understood in terms of the long lifetimes of the rotationally excited states discussed above.

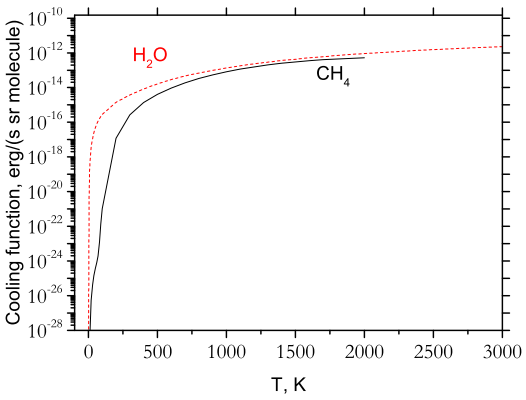


**Figure 10.** Temperature-dependent cooling functions for methane and water.

It should be noted that the cooling function of CaH is expected to underestimate at $T > 2000$ K) due to the absence of the excited electronic state in the ExoMol line list (Yadin et al. 2012). In general at high temperatures the cooling functions will be too low, due to the incompleteness of the underlying line lists. However it is possible to

give an improved estimate, $W_{\rm corr}(T)$, using the partition function, if available:

$$W_{\rm corr}(T) = W(T)\frac{Q(T)}{Q_{\rm LL}(T)} \tag{4}$$

where $Q_{\rm LL}(T)$ is the partition function obtained by summing over the energy levels used to construct the cooling function, and $Q(T)$ is converged high-temperature partition function. Good high-temperature partition functions are available for certain key molecules such as $H_3^+$ (Neale & Tennyson 1995), water (Vidler & Tennyson 2000), ammonia and phosphine (Sousa-Silva et al. 2014), and methane (Wenger et al. 2008); the compilations made for HITRAN have also proved to be reliable up to 3000 K (Gamache et al. 2000, Laraia et al. 2011). Thus, for example, Eq. (4) should probably be used to scale the cooling function given for methane in Fig. 10 since the 10to10 line list used to construct this function is incomplete for $1500 < T < 2000$ K.

## 6. Discussion and Conclusion

We have shown that by using extensive spectroscopic line lists to compute state-dependent lifetimes, interesting and underlying behaviour of the radiative properties of molecules can be revealed. The ExoMol project is systematically constructing line lists for a variety of astrophysically important molecules. The ExoMol format has recently been extended (Tennyson et al. 2016) so that the states file can be used to capture information about each state in the molecule; this includes its computed lifetime. Lifetime data for the molecules considered here can be found on the ExoMol website (www.exomol.com) and lifetime data for other molecules will be placed there as it becomes available. In particular, the importance of lifetime cooling effects for $H_3^+$ were discussed in the introduction. However, despite there being an extensive $H_3^+$ linelist being available (Neale et al. 1996), we have chosen not to present data for this system. For technical reasons the available linelist, despite its proven accuracy (Pavanello et al. 2012), does not include the weak, "forbidden", far infrared pure rotational transitions which govern both lifetime effects for states in the vibrational ground state and the cooling function at low temperatures. A new, more complete linelist for $H_3^+$ is currently being computed as part of the ExoMol project (Mizus et al. 2016). This new linelist will be used to both calculate state-dependent lifetimes and a new cooling curve.

Lifetimes also provide an important link with laboratory experiments. Many astronomically important species and/or transitions can only be reproduced in the laboratory in non-equilibrium conditions. This makes it very difficult to measure transition intensities. The alternative approach of measuring lifetimes has the advantage that it does not depend on the level populations or thermaisation of the sample being studied. More of such measurements would be very helpful for comparison and validation of our calculations.

We have shown that the presence of complex electronic spectra is responsible for a non-monotonic behaviour of $W(T)$ at low temperatures and strong cooling at high

temperatures. We will generate cooling functions routinely on the grid of 1 K and provide them together with the partition functions as part of the ExoMol database.

## Acknowledgements

This work was supported by the ERC under the Advanced Investigator Project 267219.

## References

Abel T, Bryan G L & Norman M L 2002 *Science* **295**, 93–98.
Banerjee D P K, Ashok N M, Launila O, Davis C J & Varricatt W P 2004 *Astrophys. J.* **610**, L29–L32.
Banerjee D P K, Varricatt W P, Mathew B, Launila O & Ashok N M 2012 *Astrophys. J. Lett.* **753**, L20.
Barber R J, Tennyson J, Harris G J & Tolchenov R N 2006 *Mon. Not. R. Astron. Soc.* **368**, 1087–1094.
Barton E J, Yurchenko S N & Tennyson J 2013 *Mon. Not. R. Astron. Soc.* **434**, 1469–1475.
Benson A J 2010 *Phys. Rep.* **495**, 33.
Boudon V, Pirali O, Roy P, Brubach J B, Manceron L & Auwera J V 2010 *J. Quant. Spectrosc. Radiat. Transf.* **111**, 1117–1129.
Bromm V, Yoshida N, Hernquist L & McKee C F 2009 *Nature* **459**, 49.
Cho S H, Chung H S, Kim H G, Kim H R, Roh D G & Jung J H 2009 *Astrophys. J. Suppl.* **181**, 421–432.
Cole A R H & Honey F R 1975 *J. Mol. Spectrosc.* **55**, 492–494.
Coppola C M, Lodi L & Tennyson J 2011 *Mon. Not. R. Astron. Soc.* **415**, 487–493.
Cotton W D, Ragland S, Pluzhnik E A, Danchi W C, Traub W A, Willson L A & Lacasse M G 2010 *Astrophys. J. Suppl.* **188**, 506–525.
Dagdigian P J, Cruse H W & Zare R N 1975 *J. Chem. Phys.* **62**, 1824–1833.
Deguchi S, Fujii T, Glass I, Imai H, Ita Y, Izumiura H, Kameya O, Miyazaki A, Nakada Y & Nakashima J 2004 *Publ. Astron. Soc. Jpn.* **56**, 765–802.
Dello Russo N, Bonev B P, DiSanti M A, Gibb E L, Mumma M J, Magee-Sauer K, Barber R J & Tennyson J 2005 *Astrophys. J.* **621**, 537–544.
Dello Russo N, DiSanti M A, Magee-Sauer K, Gibb E L, Mumma M J, Barber R J & Tennyson J 2004 *Icarus* **168**, 186–200.
Engel E A, Doss N, Harris G J & Tennyson J 2005 *Mon. Not. R. Astron. Soc.* **357**, 471–477.
Gamache R R, Kennedy S, Hawkins R & Rothman L S 2000 *J. Molec. Struct.* **517**, 407–425.
Goto M, McCall B J, Geballe T R, Usuda T, Kobayashi N, Terada H & Oka T 2002 *Publ. Astron. Soc. Japan* **54**, 951–961.
Gray M 1999 *Phil. Trans. Royal Soc. London A* **357**, 3277–3298.
Gray M 2012 *Maser Sources in Astrophysics* Cambridge Astrophysics Series Cambridge University Press.
Hilico J C, Loëte M, Champion J P & Destombes J L 1997 *J. Mol. Spectrosc.* **122**, 381–389.
Hirota T, Kim M K & Honma M 2012 *Astrophys. J.* **757**, L1.
Johnson S E, Capelle G & Broida H P 1972 *J. Chem. Phys.* **56**, 663–665.
Kaminski T, Schmidt M R & Menten K M 2013 *Astron. Astrophys.* **549**, A6.
Knecht D J, Pike C P, Murad E & Rall D L A 1996 *J. Spacecrafts Rockets* **33**, 677–685.
Koskinen T T, Aylward A D & Miller S 2007 *Nature* **450**, 845–848.
Krechel H, Krohn S, Lammich L, Lange M, Levin J, Scheffel M, Schwalm D, Tennyson J, Vager Z, Wester R, Wolf A & Zajfman D 2002 *Phys. Rev. A* **66**, 052509.
Kreckel H, Schwalm D, Tennyson J, Wolf A & Zajfman D 2004 *New J. Phys* **6**, 151.
Kyuberis A A, Polyansky O L, Lodi L, Tennyson J, Ovsyannikov R I & Zobov N 2016 *Mon. Not. R. Astron. Soc.* .
Lacy J H, Carr J S, Evans N J, Baas F, Achtermann J M & Arens J F 1991 *Astrophys. J.* **376**, 556–560.
Laraia A L, Gamache R R, Lamouroux J, Gordon I E & Rothman L S 2011 *Icarus* **215**, 391–400.

Le Roy R J 2007 *LEVEL 8.0 A Computer Program for Solving the Radial Schrödinger Equation for Bound and Quasibound Levels* University of Waterloo Chemical Physics Research Report CP-663 `http://leroy.uwaterloo.ca/programs/`.

Lengsfield B H & Liu B 1982 *J. Chem. Phys.* **77**, 6083–6089.

Li G, Gordon I E, Rothman L S, Tan Y, Hu S M, Kassi S, Campargue A & Medvedev E S 2015 *Astrophys. J. Suppl.* **216**, 15.

Li J, An T, Shen Z Q & Miyazaki A 2010 *Astrophys. J.* **720**, L56–L61.

Lodi L, Tennyson J & Polyansky O L 2011 *J. Chem. Phys.* **135**, 034113.

Lodi L, Yurchenko S N & Tennyson J 2015 *Mol. Phys.* **113**, 1559–1575.

McIntosh G C & Hayes A M 2008 *Astrophys. J.* **678**, 1324–1328.

Medvedev E S, Meshkov V V, Stolyarov A V & Gordon I E 2015 *J. Chem. Phys.* . (in press).

Miani A & Tennyson J 2004 *J. Chem. Phys.* **120**, 2732–2739.

Miller S, Stallard T, Melin H & Tennyson J 2010 *Faraday Discuss.* **147**, 283–291.

Miller S, Stallard T, Tennyson J & Melin H 2013 *J. Phys. Chem. A* **117**, 96339643.

Mizus I I, Alijah A, Zobov N F, Tennyson J & Polyansky O L 2016 *Mon. Not. R. Astron. Soc.* .

Neale L, Miller S & Tennyson J 1996 *Astrophys. J.* **464**, 516–520.

Neale L & Tennyson J 1995 *Astrophys. J.* **454**, L169–L173.

Neufeld D A & Melnick G J 1991 *Astrophys. J.* **368**, 215–230.

Oka T, Geballe T R, Goto M, Usuda T & McCall B J 2005 *Astrophys. J.* **632**, 882–893.

Oldani M, Andrist M, Bauder A & Robiette A G 1985 *J. Mol. Spectrosc.* **110**, 93–105.

Patrascu A T, Hill C, Tennyson J & Yurchenko S N 2014 *J. Chem. Phys.* **141**, 144312.

Patrascu A T, Tennyson J & Yurchenko S N 2015 *Mon. Not. R. Astron. Soc.* **449**, 3613–3619.

Paulose G, Barton E J, Yurchenko S N & Tennyson J 2015 *Mon. Not. R. Astron. Soc.* **454**, 1931–1939.

Pavanello M, Adamowicz L, Alijah A, Zobov N F, Mizus I I, Polyansky O L, Tennyson J, Szidarovszky T, Császár A G, Berg M, Petrignani A & Wolf A 2012 *Phys. Rev. Lett.* **108**, 023002.

Pavlyuchko A I, Yurchenko S N & Tennyson J 2015*a* *Mon. Not. R. Astron. Soc.* **452**, 1702–170.

Pavlyuchko A I, Yurchenko S N & Tennyson J 2015*b* *Mol. Phys.* **113**, 1559–1575.

Polyansky O L, Bielska K, Ghysels M, Lodi L, Zobov N F, Hodges J T & Tennyson J 2015 *Phys. Rev. Lett.* **114**, 243001.

Rivlin T, Lodi L, Yurchenko S N, Tennyson J & Le Roy R J 2015 *Mon. Not. R. Astron. Soc.* **451**, 5153–5157.

Rothman L S, Gordon I E, Babikov Y, Barbe A, Benner D C, Bernath P F, Birk M, Bizzocchi L, Boudon V, Brown L R, Campargue A, Chance K, Cohen E A, Coudert L H, Devi V M, Drouin B J, Fayt A, Flaud J M, Gamache R R, Harrison J J, Hartmann J M, Hill C, Hodges J T, Jacquemart D, Jolly A, Lamouroux J, Le Roy R J, Li G, Long D A, Lyulin O M, Mackie C J, Massie S T, Mikhailenko S, Müller H S P, Naumenko O V, Nikitin A V, Orphal J, Perevalov V, Perrin A, Polovtseva E R, Richard C, Smith M A H, Starikova E, Sung K, Tashkun S, Tennyson J, Toon G C, Tyuterev V G & Wagner G 2013 *J. Quant. Spectrosc. Radiat. Transf.* **130**, 4 – 50.

Schwalm D, Shafir D, Novotny S, Buhr H, Altevogt S, Faure A, Grieser M, Harvey A G, Heber O, Hoffmann J, Kreckel H, Lammich L, Nevo I, Pedersen H B, Rubinstein H, Schneider I F, Tennyson J, Wolf A & Zajfman D 2011 *J. Phys. Conf. Ser.* **300**.

Shuman E S, Barry J F & DeMille D 2010 *Nature* **467**(7317), 820–823.

Sousa-Silva C, Al-Refaie A F, Tennyson J & Yurchenko S N 2015 *Mon. Not. R. Astron. Soc.* **446**, 2337–2347.

Sousa-Silva C, Hesketh N, Yurchenko S N, Hill C & Tennyson J 2014 *J. Quant. Spectrosc. Radiat. Transf.* **142**, 66–74.

Sriramachandran P, Viswanathan B & Shanmugavel R 2013 *Sol. Phys.* **286**, 315–326.

Surmick D M & Parigger C G 2014 *Appl. Spectrosc.* **68**, 992–996.

Tennyson J, Hill C & Yurchenko S N 2013 *in* '$6^{th}$ international conference on atomic and molecular data and their applications ICAMDATA-2012' Vol. 1545 of *AIP Conference Proceedings* AIP, New York pp. 186–195.

Tennyson J, Kostin M A, Barletta P, Harris G J, Polyansky O L, Ramanlal J & Zobov N F 2004 *Comput. Phys. Commun.* **163**, 85–116.

Tennyson J & Yurchenko S 2016 *Exp. Astron.* .

Tennyson J & Yurchenko S N 2012 *Mon. Not. R. Astron. Soc.* **425**, 21–33.

Tennyson J, Yurchenko S N & The ExoMol team 2016 *J. Mol. Spectrosc.* .

Vidler M & Tennyson J 2000 *J. Chem. Phys.* **113**, 9766–9771.

Weck P F, Stancil P C & Kirby K 2003 *J. Chem. Phys.* **118**(22), 9997–10005.

Wenger C, Champion J P & Boudon V 2008 *J. Quant. Spectrosc. Radiat. Transf.* **109**, 2697–2706.

Wishnow E H, Orton G S, Ozier I & Gush H P 2007 *J. Quant. Spectrosc. Radiat. Transf.* **103**, 102–117.

Yadin B, Vaness T, Conti P, Hill C, Yurchenko S N & Tennyson J 2012 *Mon. Not. R. Astron. Soc.* **425**, 34–43.

Yorke L, Yurchenko S N, Lodi L & Tennyson J 2014 *Mon. Not. R. Astron. Soc.* **445**, 1383–1391.

Yurchenko S N, Blissett A, Asari U, Vasilios M, Hill C & Tennyson J 2015 *Mon. Not. R. Astron. Soc.* .

Yurchenko S N, Lodi L, Tennyson J & Stolyarov A V 2015 *Comput. Phys. Commun.* .

Yurchenko S N & Tennyson J 2014 *Mon. Not. R. Astron. Soc.* **440**, 1649–1661.

Yurchenko S N, Tennyson J, Bailey J, Hollis M D J & Tinetti G 2014 *Proc. Nat. Acad. Sci.* **111**, 9379–9383.

Yurchenko S N, Thiel W & Jensen P 2007 *J. Mol. Spectrosc.* **245**, 126–140.